REGULAR ARTICLE

blood advances

Gfi1aa and Gfi1b set the pace for primitive erythroblast differentiation from hemangioblasts in the zebrafish embryo

Chris Moore,[1,*] Joanna L. Richens,[1,*] Yasmin Hough,[1,*] Deniz Ucanok,[1] Sunir Malla,[2] Fei Sang,[2] Yan Chen,[3,4] Stone Elworthy,[3,4] Robert N. Wilkinson,[3,4] and Martin Gering[1]

[1]School of Life Sciences and [2]Deep Seq, School of Life Sciences, Queen's Medical Centre, University of Nottingham, Nottingham, United Kingdom; [3]Department of Infection, Immunity & Cardiovascular Disease, Medical School, and [4]Bateson Centre, University of Sheffield, Sheffield, United Kingdom

Key Points

- Gfi1aa and Gfi1b suppress endothelial and promote late erythroid gene expression in immature primitive erythroblasts.
- In their absence, primitive erythroblast differentiation from mesenchymal hemangioblasts is severely delayed, but not completely blocked.

The transcriptional repressors Gfi1(a) and Gfi1b are epigenetic regulators with unique and overlapping roles in hematopoiesis. In different contexts, Gfi1 and Gfi1b restrict or promote cell proliferation, prevent apoptosis, influence cell fate decisions, and are essential for terminal differentiation. Here, we show in primitive red blood cells (prRBCs) that they can also set the pace for cellular differentiation. In zebrafish, prRBCs express 2 of 3 zebrafish Gfi1/1b paralogs, Gfi1aa and Gfi1b. The recently identified zebrafish *gfi1aa* gene trap allele *qmc551* drives erythroid green fluorescent protein (GFP) instead of Gfi1aa expression, yet homozygous carriers have normal prRBCs. prRBCs display a maturation defect only after splice morpholino-mediated knockdown of Gfi1b in $gfi1aa^{qmc551}$ homozygous embryos. To study the transcriptome of the Gfi1aa/1b double-depleted cells, we performed an RNA-Seq experiment on GFP-positive prRBCs sorted from 20-hour-old embryos that were heterozygous or homozygous for $gfi1aa^{qmc551}$, as well as *wt* or morphant for *gfi1b*. We subsequently confirmed and extended these data in whole-mount in situ hybridization experiments on newly generated single- and double-mutant embryos. Combined, the data showed that in the absence of Gfi1aa, the synchronously developing prRBCs were delayed in activating late erythroid differentiation, as they struggled to suppress early erythroid and endothelial transcription programs. The latter highlighted the bipotent nature of the progenitors from which prRBCs arise. In the absence of Gfi1aa, Gfi1b promoted erythroid differentiation as stepwise loss of *wt gfi1b* copies progressively delayed Gfi1aa-depleted prRBCs even further, showing that Gfi1aa and Gfi1b together set the pace for prRBC differentiation from hemangioblasts.

Introduction

During vertebrate embryogenesis, blood cells form from the mesoderm in distinct waves of hematopoiesis.[1-4] During the primitive wave, primitive red blood cells (prRBCs) arise from mesenchymal hemangioblasts, bipotent progenitors for blood and endothelial cells (ECs).[5] The following waves develop from epithelial, hemogenic endothelial cells (HECs) that undergo endothelial to hematopoietic transition (EHT).[6-15] They give rise to predefinitive blood progenitors and definitive hematopoietic stem cells (HSCs) that maintain the blood system throughout life.

In zebrafish, prRBCs and ECs form from hemangioblasts[16-20] and develop in the posterior lateral mesoderm (PLM).[21-25] PLM cells migrate to the midline to form the intermediate cell mass of the trunk and its posterior extension, the posterior blood island of the tail. In the midline, prRBCs mature and ECs form the axial trunk vessel, the dorsal aorta (DA), and the posterior cardinal vein.[25-28] Once circulation is established, HECs in the ventral wall of the DA (vDA)[29-32] generate hematopoietic stem and progenitor cells

Submitted 26 April 2018; accepted 7 September 2018. DOI 10.1182/bloodadvances.2018020156.

*C.M., J.L.R, and Y.H. contributed equally to this study.

The full-text version of this article contains a data supplement.

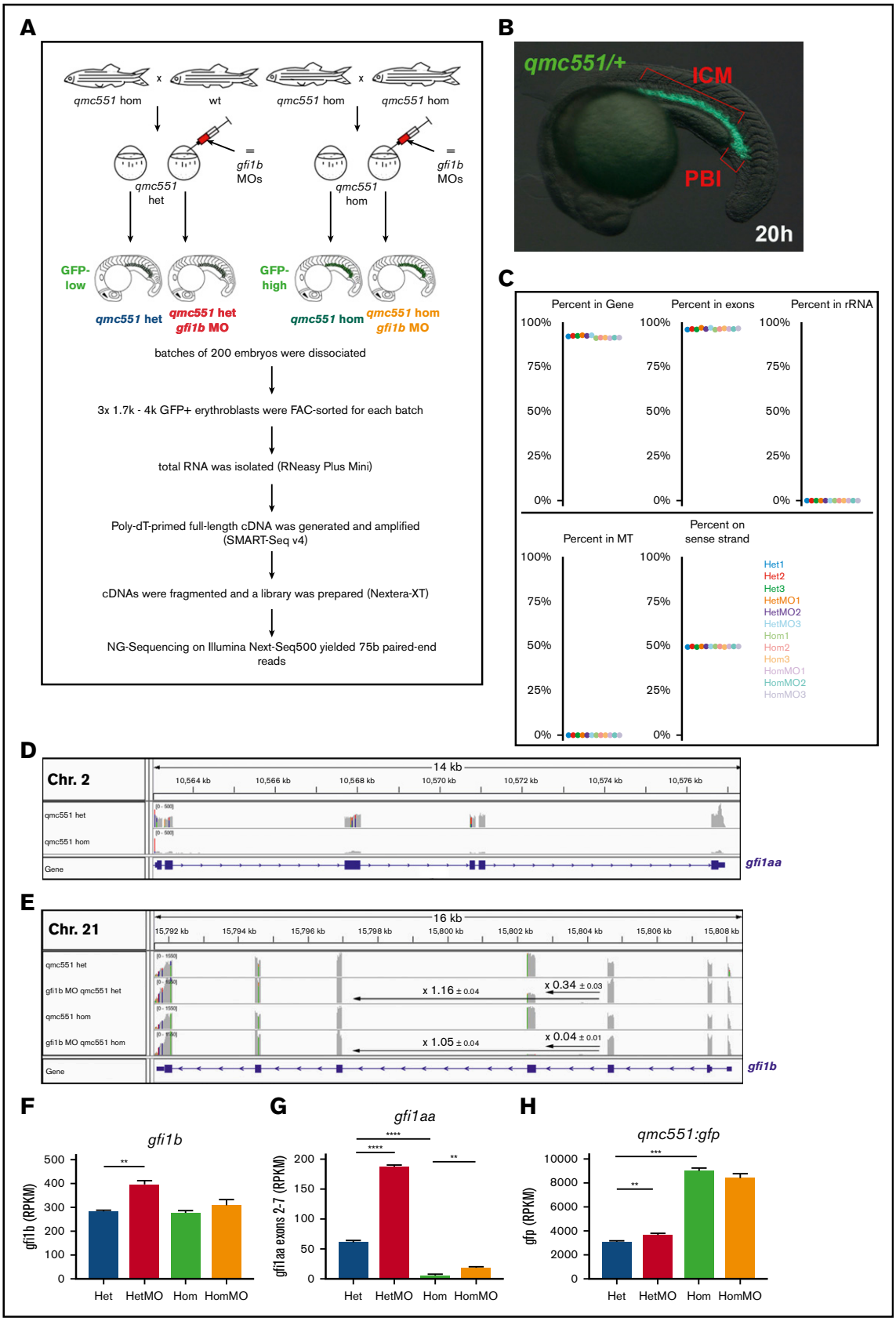

Figure 1. *Gfi1aa* and wild-type *gfi1b* transcript levels are severely reduced in primitive erythroblasts of *qmc551* homozygous and *gfi1b* MO-injected zebrafish embryos, respectively. (A) Diagram summarizing the experimental strategy of the transcriptome analysis. (B) Image of a 20-hpf *gfi1aa*^{qmc551}het zebrafish embryo taken on a

that seed the larval caudal hematopoietic tissue (CHT) and eventually the kidney marrow (KM), the adult site of hematopoiesis.[33-36]

We recently identified the zebrafish gene trap line *qmc551*, which expresses a GFP reporter in developing prRBCs and in HECs of the vDA. The latter undergo EHT and their progeny seed the CHT and the KM.[37] In *qmc551*, the gene trap transposon is inserted in intron 1 of *gfi1aa*, 1 of 3 paralogous zebrafish *gfi1/1b* genes. While *gfi1aa* and *gfi1ab* are homologous to mouse *Gfi1*,[38,39] *gfi1b* corresponds to mouse *Gfi1b*.[40] *Gfi1/1b* genes encode transcription factors (TFs) with a conserved *N*-terminal repressor domain, called the SNAG domain, a variant linker and a conserved C-terminal Zn-finger DNA binding domain.[41-43] In mouse and humans, Gfi1/1b play multiple important roles during hematopoiesis.[44,45] In different contexts, they block or promote cell proliferation, inhibit apoptosis, influence cell fate, and ensure terminal differentiation. Here, we show that they can also determine the speed of cellular differentiation.

In the *qmc551* allele, the gene trap transposon interferes with the transcription of *gfi1aa* in embryonic and adult hematopoietic cells. Nevertheless, *qmc551* homozygous (*qmc551hom*) fish are viable and fertile,[37] probably because of functional redundancy between Gfi1/1b paralogues. In HECs of the vDA, *gfi1ab* expression is induced in the absence of Gfi1aa. In prRBCs, maturation defects are only observed upon splice-morpholino (MO)–mediated knock-down of Gfi1b in *qmc551hom* embryos.[37] Here, we combined an RNA-Seq analysis on *gfi1aa*-mutant and *gfi1b*-morphant prRBCs with whole-mount in situ hybridization (WISH) experiments on novel mutant zebrafish lines to functionally analyze the genetic interaction between *gfi1aa* and *gfi1b* during primitive erythropoiesis. Our experiments reveal that Gfi1aa and Gfi1b set the pace for prRBC differentiation.

Methods

Zebrafish experiments

Zebrafish were kept as described in the zebrafish book.[46] Genetically altered zebrafish are listed in supplemental Table 1. All animal procedures were performed under the authority of the UK Home Office project licenses 40/3457, 40/3708, 30/3356, and 30/3378.

RNA-sequencing and bioinformatics

Embryos were dissociated using Liberase Blendzyme (Roche). GFP^+ cells were isolated by fluorescence activated cell sorting and subsequently lysed as described previously.[37] Genomic DNA was eliminated using genomic DNA eliminator columns, and total RNA was isolated using RNAeasy MinElute spin columns (Qiagen). Full-length cDNA was generated and amplified using the SMART-Seq v4 Ultra Low Input RNA kit for sequencing (Takara). Sequencing libraries were prepared from full-length cDNA using Nextera XT library preparation kit (Illumina). Sequencing was done on an Illumina NextSeq500 sequencing platform using 2 × 75 bp V2 chemistry. Reads were trimmed to remove adaptor and low-quality sequences using Scythe and Sickle algorithms. The trimmed read sequences are available from the European Nucleotide Archive under accession number PRJEB25583. Trimmed reads were subsequently filtered to remove tRNA and rRNA sequences. Quality filtered reads were mapped onto the zv9 zebrafish reference genome, using TopHat. The read alignments were recorded in BAM formatted alignment files. Bam files were analyzed using the Integrative Genomics Viewer and SeqMonk. Raw and normalized read counts for each gene were calculated.[47]

Gene targeting

Gene targeting was performed using TALEN and CRISPR/Cas9 technologies.[48,49] Target sites for Cas9 were identified using the CRISPRscan algorithm.[50] Guide RNAs and Cas9 mRNA were in vitro transcribed and coinjected into 1-cell-stage embryos. For genotyping, genomic DNA was isolated from fin clips and embryos and used as a template for PCR amplification. All primers are listed in supplemental Tables 6 and 8.

Phenotype analysis

WISH, *o*-dianisidine staining, and subsequent genotyping followed published protocols.[21,51,52] Peripheral blood smears were stained with Giemsa, and kidney marrow cells were collected and analyzed on the flow cytometer, as previously described by Traver and colleagues.[53]

Results

Increased *gfi1aa* promoter activity in 20-hour-old Gfi1aa- and Gfi1aa/1b-depleted primitive erythroblasts

To reveal the deficiencies in the early programming of Gfi1aa- and/or Gfi1b-depleted prRBCs, an RNA-Seq experiment was performed on GFP^+ prRBCs isolated from 20 hours postfertilization (hpf)

Figure 1. (continued) fluorescent dissecting microscope with a fluorescein isothiocyanate filter set. Brackets highlight GFP^+ cells in the intermediate cell mass (ICM) and in the posterior blood island (PBI). (C) Quality checks performed on the sequencing reads using the SeqMonk DNA Sequence Analyzer. The analysis gives the percentage of reads that map to annotated genes and the percentage of the latter that are located in exons, as well as the percentage of reads that match ribosomal RNA (rRNA) or mitochondrial DNA (MT) sequences. As expected for paired-end reads, 50% of the reads represent the sense strand. (D) Tracks showing the number of raw base read counts over the nucleotide sequences of exons 2 to 7 of *gfi1aa* in the representative samples Het1 and Hom3. These 2 samples had similar overall numbers of sequence reads (63.1 and 64.7 million reads, respectively) and can, therefore, be compared without additional normalization. (E) Tracks showing the raw base counts over the sequence of *gfi1b* in representative samples Het1, HetMO3, Hom3, and HomMO1. For the morphant samples HetMO1-3 and HomMO1-3, raw base counts over 10 nucleotides at the end of exon 3 (EE3), the beginning of exon 4 (BE4), the end of exon 4 (EE4), and the start of exon 5 (BE5) were averaged. The ratios of BE4/EE3 and EE4/BE5 were calculated and averaged. Similarly, the ratios of BE5/EE3 were determined and averaged. The average ratios are shown above the arrows in the figure. They give a good estimate of the ratio of *gfi1b* transcripts with and without exon 4 in the 2 morphant samples. To generate the images shown in panels D-E, the BAM files were imported into the Integrated Genome Viewer (IGV_2.3.72). (F-H) Bar charts comparing the average normalized transcript levels (read per kilobase of transcript per 1 million mapped reads [RPKM values]) for *gfi1b* (F), *gfi1aa* (exons 2-7, G), and *qmc551:gfp* (*gfp* sequence only, H) in *551het*, *551hetMO*, *551hom*, and *551homMO* samples. Sequence reads over exon 1 of *gfi1aa* were excluded as they cannot be allocated unambiguously to the *gfi1aa* or the *qmc551:gfp* transcript. On GraphPad Prism, Welch's *t* test was used to examine the statistical significance of the differences between the mean expression values (*$P<.05$; **$P<.01$; ***$P<.001$; ****$P<.0001$). FAC, fluorescence-activated cell.

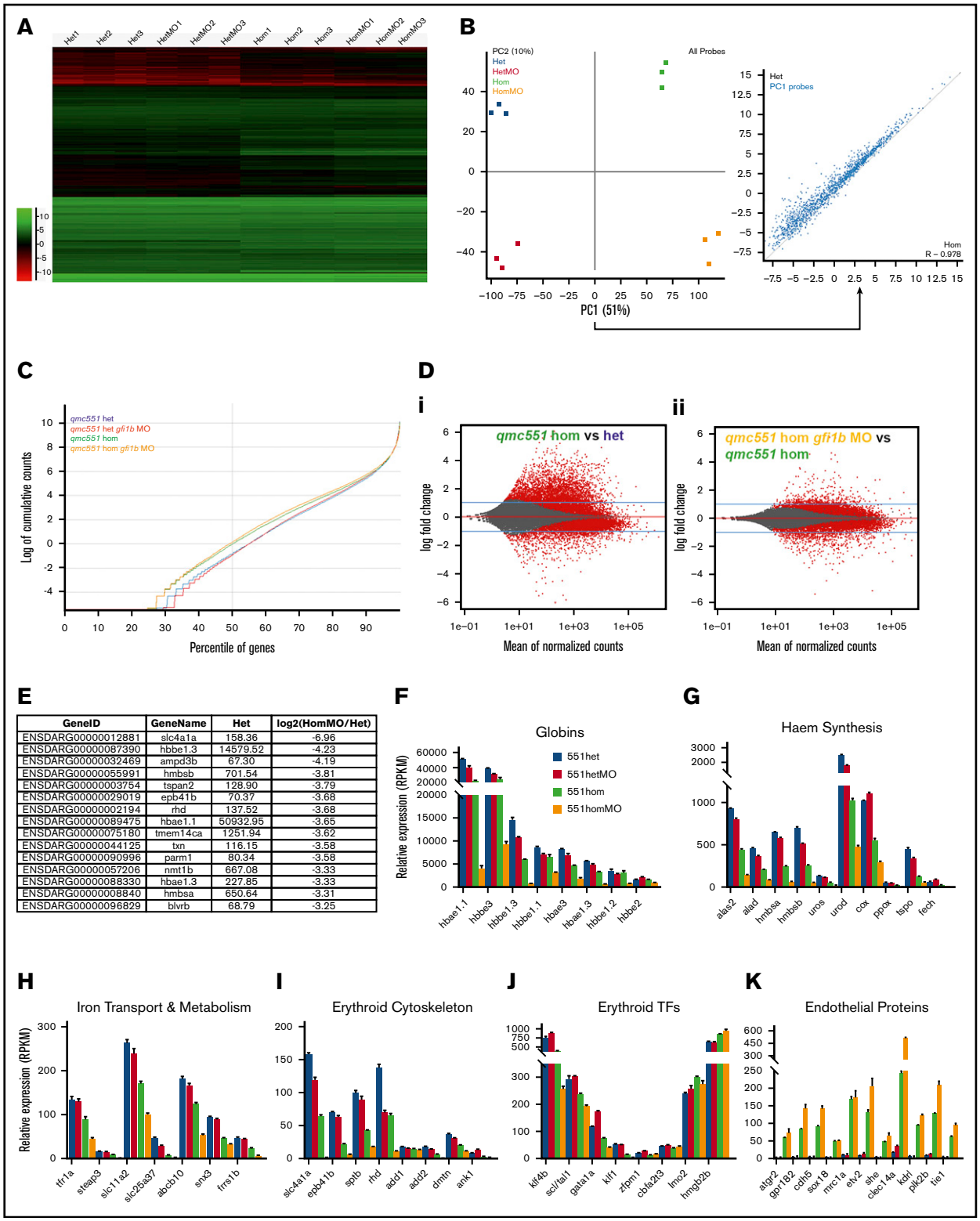

GeneID	GeneName	Het	log2(HomMO/Het)
ENSDARG00000012881	slc4a1a	158.36	-6.96
ENSDARG00000087390	hbbe1.3	14579.52	-4.23
ENSDARG00000032469	ampd3b	67.30	-4.19
ENSDARG00000055991	hmbsb	701.54	-3.81
ENSDARG00000003754	tspan2	128.90	-3.79
ENSDARG00000029019	epb41b	70.37	-3.68
ENSDARG00000002194	rhd	137.52	-3.68
ENSDARG00000089475	hbae1.1	50932.95	-3.65
ENSDARG00000075180	tmem14ca	1251.94	-3.62
ENSDARG00000044125	txn	116.15	-3.58
ENSDARG00000090996	parm1	80.34	-3.58
ENSDARG00000057206	nmt1b	667.08	-3.33
ENSDARG00000088330	hbae1.3	227.85	-3.33
ENSDARG00000008840	hmbsa	650.64	-3.31
ENSDARG00000096829	blvrb	68.79	-3.25

Figure 2. Misregulation of hundreds of genes in Gfi1aa/Gfi1b-depleted primitive erythroblasts isolated from 20 hpf zebrafish embryos. (A) Hierarchical clustering of gene expression data determined for 3 replicate *qmc551het*, *qmc551hetMO*, *qmc551hom*, and *qmc551homMO* samples. The analysis included the 9785 genes that a DESeq2 analysis had identified as differentially expressed in *qmc551het* and *qmc551homMO* prRBCs. The Log2 values of the normalized expression counts are given. (B) Principal component analysis performed on the complete data set of 24 914 genes. The set of 1610 genes that made up principal component 1 allowed the distinction of *qmc551het* and *qmc551hom* samples. The scatterplot shown in the inset compares the average expression of these genes in *551het* and *551hom* samples. (C) The distribution of reads was analyzed by plotting the cumulative read counts for 4 representative samples (*qmc551het1*, *qmc551hetMO3*, *qmc551hom3*, and *qmc551homMO1*)

L

GeneID	GeneName	Hom/Het	log2(Hom/Het)
ENSDARG00000035552	agtr2	28.62	4.84
ENSDARG00000036616	gpr182	23.26	4.54
ENSDARG00000075549	cdh5	18.19	4.18
ENSDARG00000058598	sox18	17.74	4.15
ENSDARG00000073928	mrc1a	16.82	4.07
ENSDARG00000053868	etv2	16.21	4.02
ENSDARG00000037895	ramp2	15.83	3.98
ENSDARG00000043376	egfl7	15.75	3.98
ENSDARG00000087956	she	15.36	3.94
ENSDARG00000027966	ap1s3b	15.19	3.92
ENSDARG00000026751	clec14a	14.72	3.88
ENSDARG00000015815	kdrl	14.46	3.85
ENSDARG00000093584	zgc:193505	13.67	3.77
ENSDARG00000019130	plk2b	13.57	3.76
ENSDARG00000004105	tie1	13.37	3.74

M

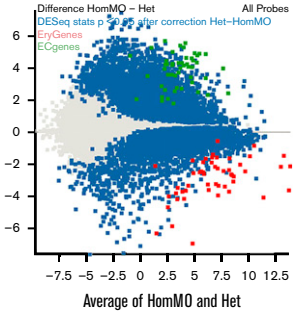

N

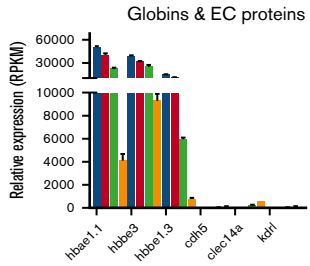

Figure 2. (Continued).

embryos that were heterozygous or homozygous for *qmc551*, as well as *wt* or morphant for *gfi1b* (Figure 1A). At this stage, qmc551:GFP fluorescence is robust and restricted to prRBCs (Figure 1B). RNA-Seq reads were mapped to the zebrafish genome. After initial quality checks (Figure 1C), we examined the relative expression of *gfi1aa* and *gfi1b* mRNAs in our samples. For this purpose, we visualized raw read count differences in samples with similar overall read counts (Figure 1D-E) and compared averaged normalized read counts calculated from all replicates (Figure 1F-G). Both sets of data showed that there is a 10-fold reduction of *gfi1aa* mRNA levels in *qmc551hom* erythroblasts relative to *qmc551het* cells (Figure 1D,G). Combined with the previous finding that *gfi1aa* mRNA levels are halved in *qmc551het* relative to *wt* blood cells,[37] this suggests that *qmc551hom* prRBCs express *gfi1aa* at 5% of the *wt* level. Although raw read counts for *gfi1b* were similar over most exons, exon 4 was an exception. Its read counts were clearly reduced in the *gfi1b*-morphant samples (Figure 1E), confirming previous reverse transcription polymerase chain reaction (RT-PCR) data on RNA isolated from embryos injected with the *gfi1b* exon 4 splice MOs.[37] The loss of exon 4 reads was almost complete in the *qmc551homMO* erythroblasts (96%), but less optimal in the *qmc551hetMO* cells (66%) (Figure 1E), most likely reflecting variability between MO injections.

While normalized *gfi1b* mRNA levels were slightly higher in *gfi1b* morphants, normalized *gfi1aa* mRNA levels were increased threefold (Figure 1G). In comparison, *qmc551:gfp* mRNA levels rose by only 19% (Figure 1H). Overall, *qmc551:gfp* mRNA was 50-fold more abundant than *gfi1aa* mRNA. Given that both transcripts initiate at the same promoter, this difference suggests differential mRNA stability. The very modest increase of *qmc551:gfp* mRNA levels in the *gfi1b*-morphant prRBCs suggests that the rise in *gfi1aa* promoter activity was a recent event that is masked in the *gfp* data by the abundance of preexisting stable *gfp* mRNA. In the *qmc551hom* samples, *gfp* mRNA levels were threefold higher than in the *qmc551het* samples. This is more than one would expect from a gene dosage effect and may suggest autoregulation of the *gfi1aa* promoter.

Increased endothelial and decreased erythroid gene expression in 20-hour-old Gfi1aa single- and Gfi1aa/Gfi1b double-depleted primitive erythroblasts

Next, global differences in gene expression were examined. Hierarchical clustering showed that the gene expression changes clearly partitioned the samples into the replicate sets (Figure 2A). A principal component analysis revealed that the gene expression differences between *qmc551het* and *qmc551hom* prRBCs were more pronounced than those caused by the absence of Gfi1b (Figure 2B). Principal component 1, which was responsible for most of the variation in the data set, consisted of genes with reduced expression in Gfi1aa-depleted prRBCs (Figure 2B inset). However, not all differentially expressed genes were downregulated in *qmc551hom* prRBCs. Plotting cumulative raw read counts over the percentile of genes arranged in the order of ascending average expression revealed a remarkable increase in read counts in low to medium expressed genes in *qmc551hom* relative to *qmc551het* samples (Figure 2C). Advanced count-based statistics using the DESeq2 method[54] confirmed the statistical significance of the described gene expression changes (Figure 2Di). Additional depletion

Figure 2. (continued) over the percentiles of genes arranged in the order of ascending average gene expression. (D) A DESeq2 analysis had identified differentially expressed genes among the 24 914 genes analyzed. Here, MA plots (mean fold change over average expression) are shown that report M, the log2 value of the ratio of Hom/Het (left) and of HomMO/Hom (right), over panel A, the log2 value of the average expression in all Hom+Het (left) and HomMO+Hom values (right), for all of the 24 914 genes. All differentially expressed genes are shown in red. These were 8426 and 5081 in Di and Dii, respectively. The MA plot was generated using Bioconductor. (E) List of the top 15 genes with the highest fold decrease in expression in *qmc551homMO* vs *qmc551het* samples and an average expression of at least 60 RPKM in *qmc551het* prRBCs. (F-K) Bar charts comparing the normalized average expression levels of the named erythroid and endothelial genes in *qmc551het*, *qmc551hetMO*, *qmc551hom*, and *qmc551homMO* prRBCs. The standard deviations are shown. (L) List of the top 15 genes with the highest fold increase in expression in *qmc551hom* relative to *qmc551het* samples and an RPKM value of at least 40 in the *qmc551hom* prRBCs. (M) MA plot plotting genes based on their average expression in *qmc551homMO* and *qmc551het* and the mean of the ratio of average *qmc551homMO* to average *qmc551het* expression values. Genes are colored in blue when the DESeq2 statistical analysis showed that the differences in raw read counts were significantly different in *qmc551homMO* and *qmc551het* prRBCs. Typical endothelial and erythroid genes are highlighted in green and red, respectively. These genes are listed in supplemental Table 5. (N) Bar chart comparing the average normalized expression of the named globin and endothelial protein genes in all 4 sets of replicates. Standard deviations are shown. The bar color coding used in panels F-K and N is explained in panel F.

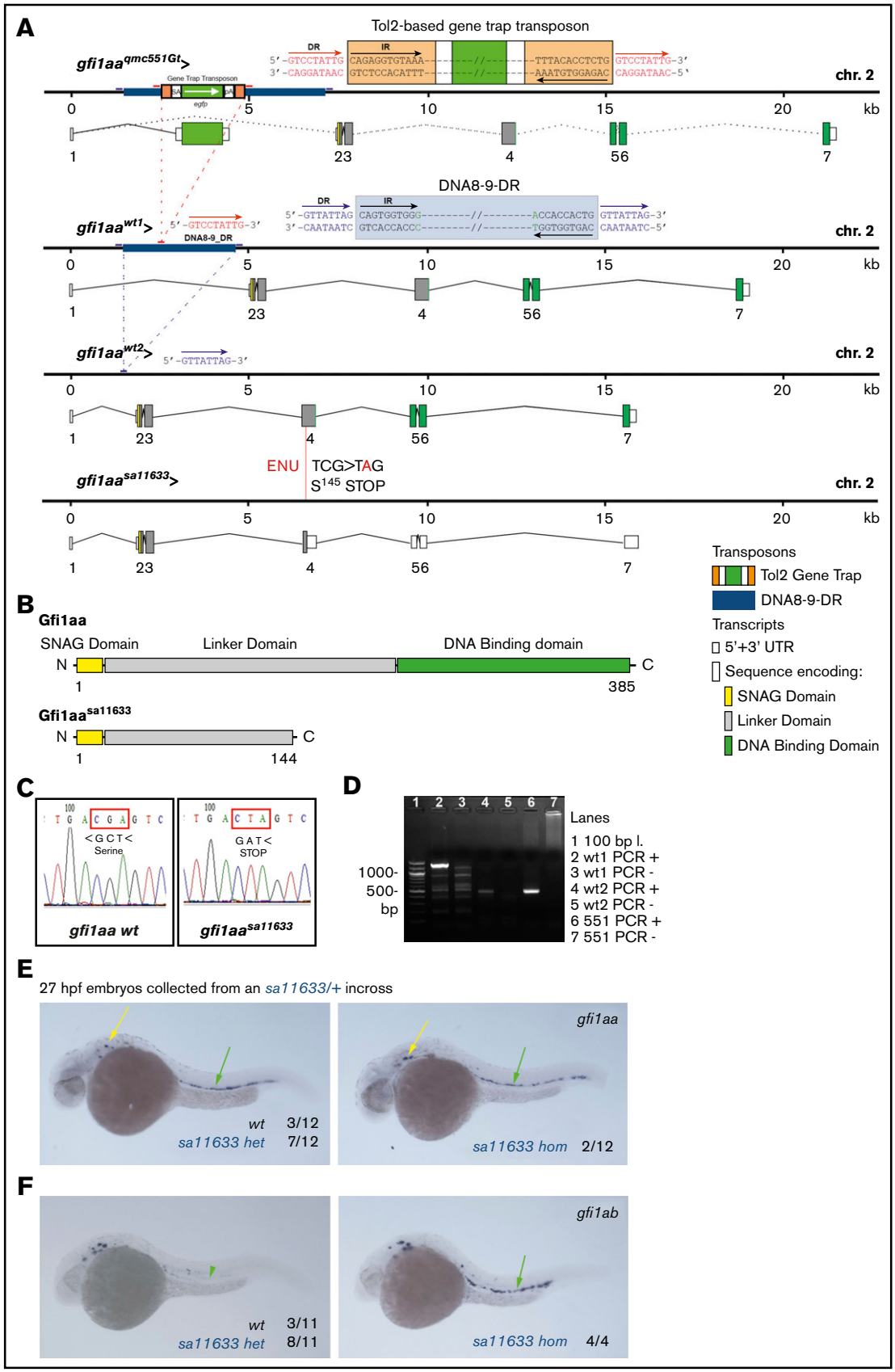

Figure 3.

of Gfi1b expression had a notable but milder effect on gene expression (Figure 2Dii).

Many of the downregulated genes represented late erythroid genes (Figure 2E; supplemental Figure 1). In addition to the globin genes (Figure 2F), they included genes for proteins involved in heme synthesis, iron transport and metabolism, and components of the special erythroid cytoskeleton (Figure 2E-I). Although some TFs known to drive erythroid gene expression were also downregulated, others were relatively unaffected (Figure 2J). Overall, the downregulation of genes appeared to affect all aspects of RBC biology (supplemental Figure 1F).

Many of the upregulated genes encoded proteins with well-defined roles in ECs (Figure 2K-L). Overall, the effects on blood and EC gene expression were mild in *gfi1b*-morphant cells, strong in *gfi1aa*-mutant cells, and even stronger in Gfi1aa/1b-double-depleted prRBCs (Figure 2F-K). The differential expression of blood and EC genes (Figure 2M) does not indicate that the Gfi1aa/1b-depleted prRBCs were reprogrammed to be ECs. First, some erythroid genes were still expressed at levels much higher than any EC gene (Figure 2N). Second, the qmc551: GFP^+ cells retained their mesenchymal character and entered circulation when the primary circulatory loop was established.[37] Thus, the cells were clearly prRBCs, blocked or delayed in erythroid maturation.

Characterization of novel *gfi1aa* and *gfi1b* alleles

Next, we validated the transcriptome data in WISH experiments performed on *gfi1aa* and *gfi1b* single- and double-mutant embryos. For this purpose, we characterized an additional *gfi1aa*-mutant (Figure 3, color-coded blue) and generated 2 new *gfi1b*-mutant lines (Figure 4, color-coded red). The $gfi1aa^{sa11633}$ allele had previously been identified in an ethylnitrosourea mutagenesis screen[55] and carries a nonsense mutation in exon 4 of *gfi1aa* (Figure 3A). The 2 novel *gfi1b* alleles were generated using TALEN and CRISPR/Cas9 technologies. The TALEN-induced $gfi1b^{sh339}$ allele harbors a frameshift mutation in exon 3, the $gfi1b^{qmc554}$ allele a CRISPR/Cas9-induced deletion, and frameshift mutation in exon 4 (Figure 4A).

The 3 mutant alleles encode truncated Gfi1aa/1b proteins (Figures 3B and 4B). They possess an *N*-terminal SNAG domain, vary in the length of the retained linker, and lack the Zn-finger DNA-binding domain and are, therefore, likely to represent severe loss-of-function alleles. DNA sequencing reveals the differences between the *gfi1aa/1b wt* and the mutant $gfi1aa^{sa11633}$ and $gfi1b^{sh339}$ alleles (Figures 3C and 4C). PCR amplification of allele-specific fragments identifies the $gfi1aa^{qmc551}$ and $gfi1b^{qmc554}$ alleles (Figures 3D and 4D).

When we set up the PCR genotyping assay for $gfi1aa^{qmc551}$, we detected 2 different *gfi1aa wt* alleles, which differed in the length of intron 1 (Figure 3A). One allele (*wt1*) corresponds to the Zv9 reference sequence. The shorter second allele (*wt2*) lacks the sequence of the nonautonomous transposon DNA8-9-DR. While the $gfi1aa^{sa11633}$ allele carries the short intron 1, $gfi1aa^{qmc551}$ possesses the long intron. In $gfi1aa^{qmc551}$, the gene trap transposon integrated into an existing transposon, highlighting that the first intron of *gfi1aa* is a highly accessible DNA sequence.

The loss of *gfi1aa* transcription caused by the transposon integration in $gfi1aa^{qmc551}$ de-represses *gfi1ab* expression in the vDA.[37] Here, WISH experiments showed that although vDA *gfi1aa* mRNA levels are normal in $gfi1aa^{sa11633}hom$ embryos (Figure 3E), the level of *gfi1ab* mRNA was clearly increased as expected (Figure 3F).

The RNA-Seq data indicated that *gfi1aa* is upregulated in 20 hpf *gfi1b*-morphant prRBCs (Figure 1G). WISH experiments confirmed the *gfi1aa* upregulation in 20 hpf prRBCs of $gfi1b^{sh339}hom$ and $gfi1b^{qmc554}hom$ embryos (Figure 4E-F), but also revealed that it was transient, as *gfi1aa* mRNA was no longer detectable in prRBCs at 28 to 30 hpf (Figure 4G-H). $Gfi1b^{sh339}$ and $gfi1b^{qmc554}$ mRNAs themselves were stable (ie, not subject to nonsense-mediated decay; supplemental Figure 2).

Gfi1aa suppresses endothelial gene expression in early erythroid progenitors

To validate the EC gene upregulation we observed in Gfi1aa-depleted prRBCs in the RNA-Seq data, WISH experiments were performed with probes against mRNAs coding for EC membrane proteins (Cdh5, Clec14a, Sptlc2a, and Flk1/Kdrl) and TFs (Sox7 and Etv2). Initial experiments on 22 hpf embryos revealed no obvious increase in *cdh5* expression in $gfi1aa^{qmc551}hom$ prRBCs of the intermediate cell mass (Figure 5A), while *cdh5* upregulation in the less mature prRBCs of the posterior blood island was possibly masked by strong *cdh5* expression in tail ECs. To see whether prRBC progenitors of the trunk expressed EC genes earlier, younger embryos were examined. These WISH experiments provided 4 major insights. First, endothelial genes coding for membrane receptors and TFs were indeed ectopically expressed in

Figure 3. The *qmc551* and *sa11633* alleles of *gfi1aa*. (A) Genomic maps of 2 wild-type and 2 mutant alleles of *gfi1aa*, including information about transcripts and their splice products. The 2 *wt* alleles differ in intron 1. Intron 1 of allele *wt1* carries a hAT-Tol2 family transposon called DNA8-9_DR whose target site was duplicated upon integration. The duplicated sequences flank the transposon as direct repeats. In the *qmc551* allele, the gene trap transposon was inserted into the DNA8-9_DR transposon of the *wt1* allele. Please note that most $gfi1aa^{qmc551Gt}$ transcripts terminate behind the *gfp* reading frame. Splicing between the splice donor at the end of exon 1 and the splice acceptor on the gene trap transposon allows GFP expression from the *qmc551* allele.[37] The *wt2* and *sa11633* alleles do not possess transposon insertions in intron 1. Their intron 1 sequence is considerably shorter. The *sa11633* allele carries a nonsense mutation in exon 4. Detailed annotations are provided in the inset. (B) The diagram shows the full-length *wt* Gfi1aa protein with all its functional domains and the truncated Gfi1aa protein encoded by the *sa11633* allele. (C) PCR of exon 4 sequences and subsequent DNA sequencing are required to distinguish *wt* and *sa11633* alleles of *gfi1aa*. The panels show Sanger DNA sequencing reads of the template strand of the *wt* and *sa11633* alleles of *gfi1aa*. The coding sequence has been added below the sequence read. It shows that the mutation converts the serine145 codon to a premature stop codon. (D) PCR-based genotyping of *wt* and *qmc551* alleles of *gfi1aa*. In lanes 2 to 7, PCR products are shown that were amplified on genomic DNA samples that did (+) or did not (−) contain the respective *gfi1aa* allele. The expected *wt1*, *wt2*, and *qmc551* fragments are 1322, 477, and 491 bp in size. Information on primer sequences is provided in supplemental Table 8. (E-F) Lateral views of embryos stained by WISH. Yellow and green arrows point at gene expression in inner ear hair cells and in the ventral wall of the dorsal aorta, respectively. Numbers of embryos analyzed are provided on the panels.

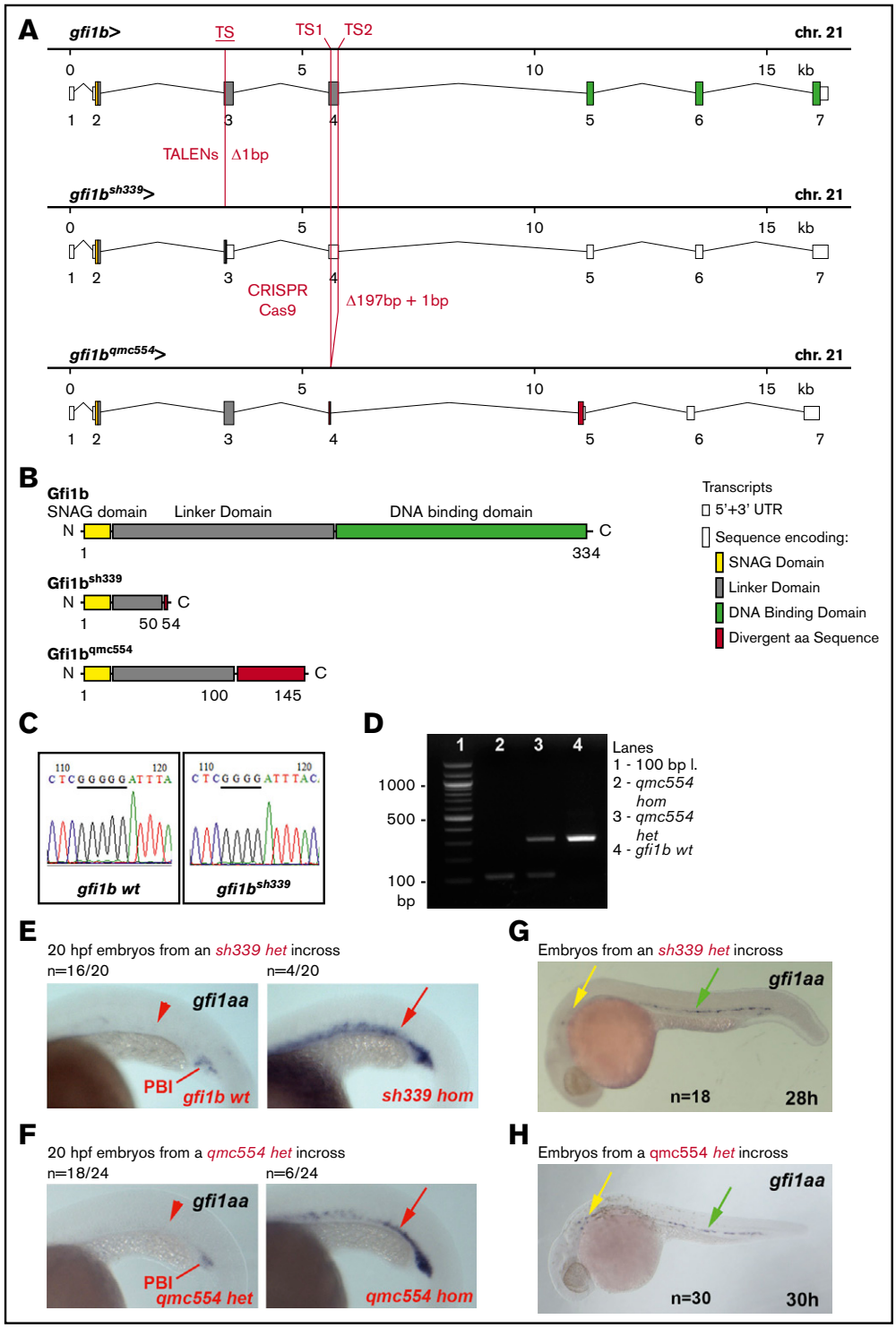

Figure 4. *The sh339* and *qmc554* alleles of *gfi1b*. (A) Genomic maps of the *wt*, *sh339*, and *qmc554* alleles of *gfi1b*, including information about transcripts and splice products. Additional annotations are provided in the inset. (B) Gfi1b protein products encoded by the *wt* and the 2 mutant *gfi1b* mutant alleles. (C) PCR amplification of exon 3 sequences and subsequent sequencing are used to identify *sh339* carriers. The panels show examples of Sanger DNA sequencing reads. A missing G in a stretch of 5 consecutive Gs on the template strand defines the *sh339* allele. As the mutation in *sh339* eliminates a *BslI* restriction site, a restriction digest can also distinguish *wt* and mutant *gfi1b* alleles. (D) PCR amplification of exon 4 sequences distinguishes the *wt* allele and the deletion allele *qmc554* of *gfi1b*. The expected *wt* and *qmc554* PCR fragments are 305 and 109 bp long. Primer sequences are provided in supplemental Table 8. (E-H) Lateral views of embryos stained by WISH. Yellow, green, and red arrows point at gene expression in inner ear hair cells, in the ventral wall of the dorsal aorta, and in prRBCs, respectively. Red arrowheads highlight the lack of gene expression in prRBCs. Genotyping of 3 of the 10 embryos with elevated *gfi1aa* expression in panels E-F revealed that they were homozygous mutants. Representative examples are shown. All embryos shown in panels G-H display the same *gfi1aa* expression pattern, irrespective of their *gfi1b* genotype.

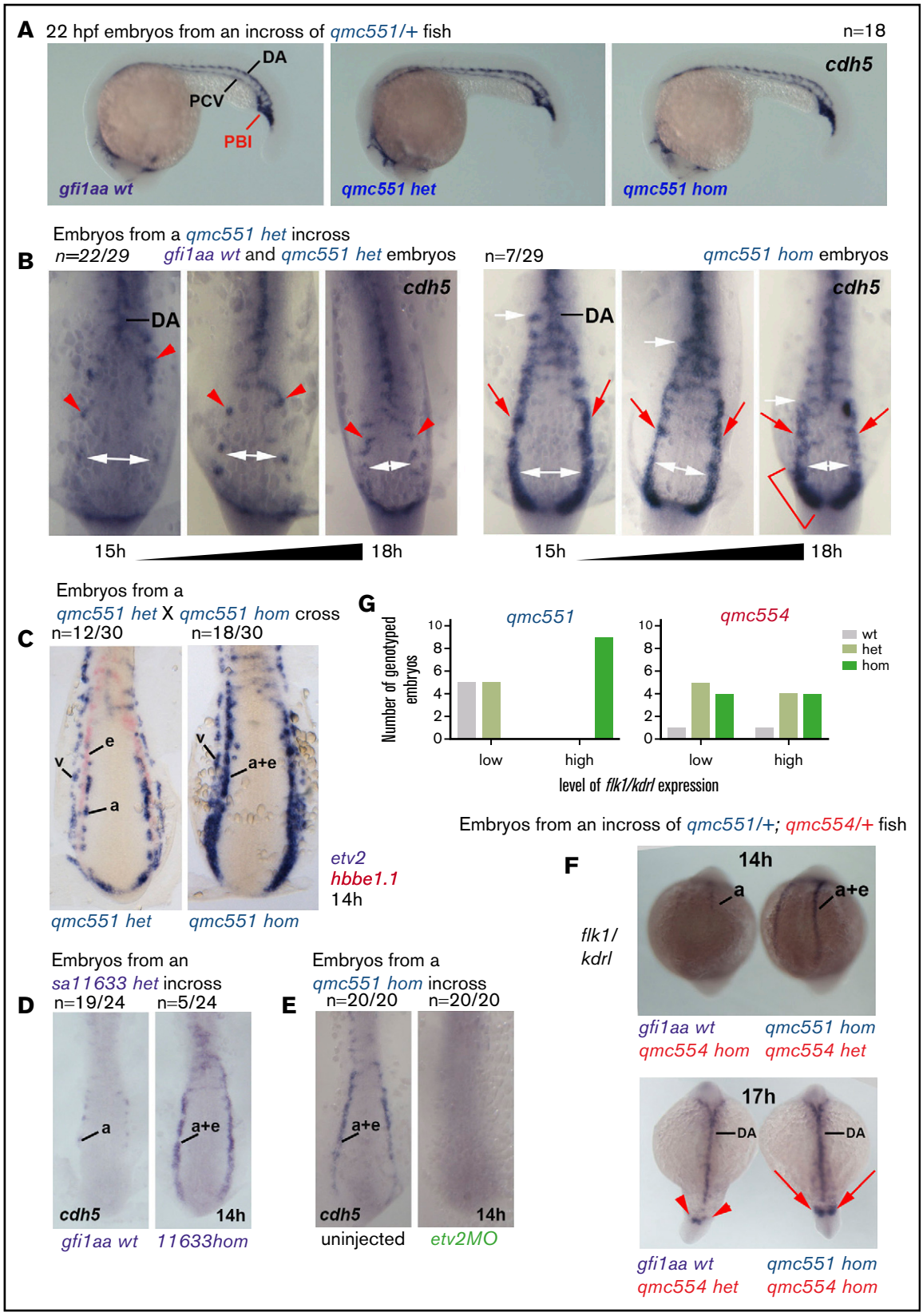

Figure 5. *Gfi1aa* suppresses the endothelial gene expression program in primitive erythroblasts developing from the posterior lateral mesoderm. The figure shows zebrafish embryos stained in WISH experiments. Lateral views of embryos are shown in panel A. Flat-mounts of the posterior parts of embryos are displayed in panels B-E. Posterior and dorsal views of embryos are presented in the top and bottom panels of F, respectively. (A) *Wt*, *gfi1aa*^{qmc551}*het*, and *gfi1aa*^{qmc551}*hom* embryos display very

prRBC progenitors in *gfi1aa*^{qmc551}*hom* and *gfi1aa*^{sa11633}*hom* embryos (Figure 5B-D; supplemental Figure 3). Second, this ectopic expression became weaker as the prRBCs started to migrate to the midline and matured (Figure 5B). Third, this ectopic expression required the endothelial TF Etv2 (Figure 5E), suggesting that in the absence of Gfi1aa, EC genes were activated in prRBCs by an EC gene regulatory network, and not by early erythroid TFs. Fourth, ectopic erythroid activation of endothelial genes did not correlate with the genotype of *gfi1b* (Figure 5F-G; supplemental Figure 3E-F). Altogether, these data suggested that Gfi1aa was expressed in early prRBC progenitors to suppress the EC gene regulatory network. In its absence, the network transiently drives the expression of endothelial markers. The final loss of EC gene expression reveals the presence of additional mechanisms to suppress EC gene expression in maturing prRBCs.

Loss of increasing numbers of *gfi1aa* and *gfi1b* gene copies causes progressive delays in erythroid maturation, but no obvious defect in definitive hematopoiesis

Next, we performed WISH experiments with probes for late erythroid genes. For this purpose, embryos were collected from incrosses of *gfi1aa*^{qmc551}/*gfi1b*^{sh339}, *gfi1aa*^{qmc551}/*gfi1b*^{qmc554}, and *gfi1aa*^{sa11633}/*gfi1b*^{sh339} double heterozygous fish. We focused on the expression of *slc4a1a*, the gene that displayed the highest fold reduction in expression in Gfi1aa/1b-depleted prRBCs (Figure 2E). Among the stained 18- to 19-hpf embryos, a quarter displayed hardly any staining. Genotyping identified these embryos as *gfi1aa*^{qmc551}*hom* or *gfi1aa*^{sa11633}*hom* mutants (Figure 6A-C). There was no obvious correlation between the level of staining and the *gfi1b* genotype (Figure 6A-C). The same experiments performed on embryos from incrosses of single heterozygous *gfi1aa*^{qmc551}, *gfi1b*^{sh339}, and *gfi1b*^{qmc554} carriers confirmed that Gfi1aa alone was important for normal *slc4a1a* expression at this stage (supplemental Figure 4).

To determine whether Gfi1aa-depleted prRBCs recovered and whether the role of Gfi1b was detectable at later stages of erythroid differentiation, the WISH experiments were repeated on 22- to 24-hpf *gfi1aa*^{qmc551}/*gfi1b*^{qmc554} embryos. At 22 to 24 hpf, the subset of embryos with very low *slc4a1a* expression was much smaller (n = 4/98) than before. All embryos in this subset were *gfi1aa*^{qmc551}/*gfi1b*^{qmc554} double homozygotes (Figure 6D; supplemental Figure 5). Embryos with slightly higher *slc4a1a* expression were *gfi1aa*^{qmc551} homozygotes that retained 1 wt copy of *gfi1b*. *Gfi1aa*^{qmc551} mutants with 2 *wt gfi1b* copies were indistinguishable from *wt* embryos. Similar observations were made with probes for 3 other late erythroid genes, *cahz*, *epor*, and *klf1* (supplemental Figure 6). These data allowed 2 conclusions: First, Gfi1aa-depleted RBCs are delayed and not blocked in differentiation, and second, Gfi1b promotes erythroid differentiation, most notably in the absence of Gfi1aa. The presence of increasing numbers of *gfi1b wt* copies promotes a progressively earlier onset of late erythroid gene expression.

Despite the initial delay, Gfi1aa-deficient prRBCs recover by 3 dpf, and only additional MO-induced loss of Gfi1b causes circulating prRBCs to carry less hemoglobin and display an immature cell morphology.[37] Similarly, prRBCs in our *gfi1aa*^{qmc551}/*gfi1b*^{qmc554} double-mutant embryos displayed less hemoglobin (Figure 6E) and were obviously hypochromic (Figure 6F). Hypochromic prRBCs were also observed in *gfi1aa*^{sa11633}/*gfi1b*^{sh339} double-mutant embryos (supplemental Figure 7). Giemsa staining of prRBCs isolated from the circulation showed that *gfi1aa*^{qmc551}/*gfi1b*^{qmc554} double-mutant cells looked more immature and carried less condensed nuclei than *wt* cells (Figure 6G-H). Nuclear condensation between days 2 and 3 revealed that cellular maturation continued in *wt* and double-mutant prRBCs. Whether the double-mutant cells completed maturation was difficult to follow once definitive RBCs (defRBCs) entered circulation on day 4.[36,56]

Figure 5. (continued) similar *cdh5* expression patterns at 22 hpf. Embryos were stained, photographed, and genotyped; 4 of 18 embryos were *gfi1aa*^{qmc551}*hom*. Representative *wt*, *gfi1aa*^{qmc551}*het*, and *gfi1aa*^{qmc551}*hom* embryos are shown. (B) The expression pattern of the endothelial gene *cdh5* is expanded in the posterior lateral mesoderm of Gfi1aa-depleted embryos. A mix of 15 to 18 hpf embryos derived from *gfi1aa*^{qmc551}*het* incross were stained for the expression of *cdh5*, flat-mounted, photographed, and genotyped. Embryo images were sorted on the basis of the level of *cdh5* expression and then arranged according to their development stage, which was judged by the distance between the bilateral PLM stripes. In younger embryos, this distance is larger than in older embryos (see white double arrows). Genotyping revealed that all *gfi1aa*^{qmc551}*hom* mutant embryos displayed expanded expression patterns for *cdh5* in the PLM when compared with wt and *gfi1aa*^{qmc551}*het* embryos. The white arrows indicate the anterior extent of the solid stripe of *cdh5*$^{+}$ cells in the PLM. Red arrowheads point at normal *cdh5* gene expression in dispersed small clusters of PLM cells in *wt* and *gfi1aa*^{qmc551}*het* embryos.[28,81] Red arrows highlight unusually robust *cdh5* expression in a solid stripe of PLM cells of *gfi1aa*^{qmc551}*hom* mutant embryos. A red bracket indicates robust *cdh5* expression in the posterior part of the PLM in the 18 hpf *gfi1aa*^{qmc551}*hom* embryo. (C) In the absence of Gfi1aa, mRNA for the endothelial transcription factor Etv2 is ectopically expressed in prRBCs. Embryos from a double WISH experiment are shown. Embryos were first stained for the presence of *etv2* mRNA in purple, and subsequently with a probe for *hbbe1.1* mRNA in red. In the *gfi1aa*^{qmc551}*het* embryos, *etv2* is expressed in 2 stripes of EC progenitors, arterial (a) progenitors medially and venous (v) progenitors laterally. This is consistent with previous findings in *wt* embryos.[25] Please note that the *hbbe1.1*-expressing primitive erythroid (e) progenitors are lateral to and much more closely associated with the arterial EC progenitors. In the *gfi1aa*^{qmc551}*hom* mutant embryos, the medial stripe of *etv2*$^{+}$ cells is wider and encompasses arterial EC progenitors and prRBCs (a+e). Please note that the purple staining in prRBCs masks any red staining that may be present. (D) The *cdh5* expression pattern is expanded in *gfi1aa*^{sa11633} homozygous mutant embryos. Embryos were stained and genotyped. Representative embryos are shown. (E) Endothelial and erythroid *cdh5* expression require the presence of the endothelial TF Etv2. Two- and 4-cell stage embryos from a *gfi1aa*^{qmc551}*hom* incross were injected with 10 ng of a previous validated *etv2* 5′ untranslated region (UTR) MO.[63,64] Embryos were collected at 14 hpf and stained by WISH. None of the morphant embryos showed any staining. An 18-hpf *wt* embryo that had been added to the batch of morphant embryos before the WISH experiment showed normal cdh5 expression in ECs (data not shown), confirming that the WISH procedure successfully detected *cdh5* mRNA. (F-G) The level of expression of the EC marker *flk1/kdrl* in the posterior lateral mesoderm correlates with the genotype of *gfi1aa*, and not with the genotype of *gfi1b*. In this experiment, *gfi1aa*^{qmc551}/*gfi1b*^{qmc554} double-heterozygous fish were incrossed. Their embryos were stained by WISH, subsequently photographed, and genotyped. Representative embryos with weak and strong staining are shown. The bar charts in (G) summarize the collective results of the *gfi1aa* and *gfi1b* genotyping performed on 14- and 17-hpf somite stage embryos that displayed low or high levels of *flk1/kdrl* expression in the PLM. The *flk1/kdrl* data support the view that the EC gene upregulation is transient in *gfi1aa* single- and *gfi1aa/1b* double-mutant embryos.

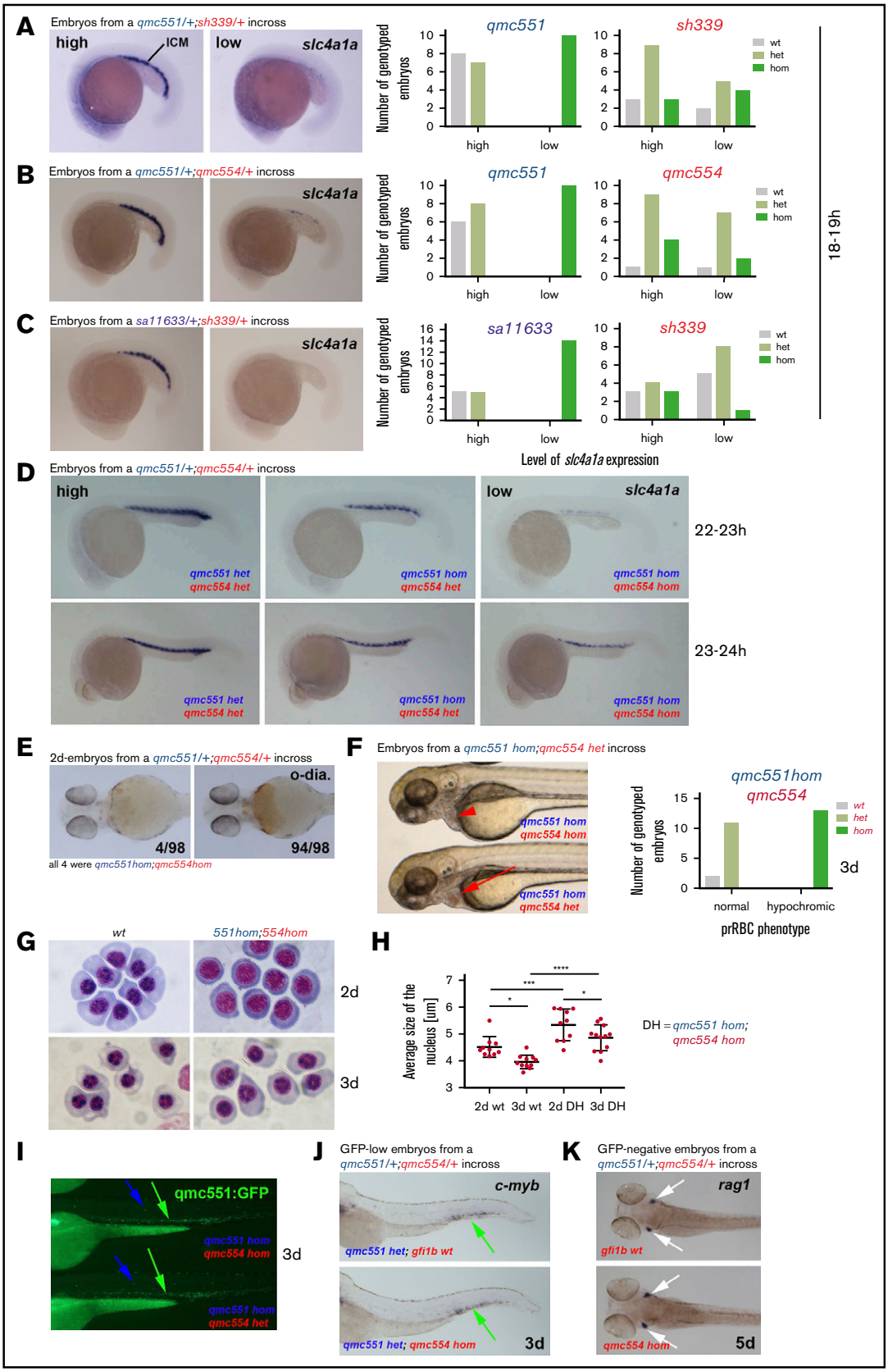

Figure 6. Primitive erythropoiesis is delayed in Gfi1aa/Gfi1b-depleted embryos. Images of embryos stained by RNA whole-mount in situ hybridization are shown in panels A-D and J-K. Embryos in panel E were stained with *o*-dianisidine. Live embryos are shown in panels F and I. Views of embryos are lateral in panels A-D,F,I,J. Ventral

Using a translation-blocking *gfi1b* MO, an unrelated study had previously suggested an essential role for Gfi1b in definitive hematopoiesis.[40] However, both our double-mutant and our *gfi1aa*-mutant, *gfi1b*-splice morphant embryos displayed normal qmc551:GFP fluorescence in the CHT (Figure 6I; supplemental Figure 8A). Furthermore, there was normal CHT *cmyb* expression on day 3 and normal *rag1* expression in thymic T-cell progenitors on day 5 in *gfi1b*^{qmc554}*hom* mutants (Figure 6J-K) and in *gfi1aa*^{qmc551}*hom gfi1b*-splice morphants (supplemental Figure 8B-C), suggesting that loss of Gfi1b alone or in combination with Gfi1aa does not interfere with the onset of definitive hematopoiesis in zebrafish.

Gfi1b single- and *gfi1aa/gfi1b* double-mutants are viable but carry abnormal erythrocytes

Embryos derived from an incross of double heterozygous *gfi1aa*^{qmc551}/*gfi1b*^{qmc554} carriers were sorted on the basis of GFP expression and raised to adulthood (Figure 7A). At 15 months, all expected genotypes were present in Mendelian ratios (Figure 7B), demonstrating that single and double mutants are viable. None of the fish showed signs of cardiomegaly, a compensatory response to pronounced anemia.[57-62] Nevertheless, peripheral RBCs of *gfi1b*^{qmc554}*hom* and *gfi1b*^{sh339}*hom* fish displayed abnormal nuclear and cellular morphology (Figure 7C; supplemental Figure 9). Flow cytometric analysis of the *gfi1b*^{qmc554}*hom* KM cells revealed abnormal forward and side scatter profiles. Relative to *wt* KM, the ratio of 2 erythroid subpopulations Ery2/Ery1 was reduced and the relative number of progenitors increased in all *gfi1b*^{qmc554}*hom* fish (Figure 7D-F). Overall, however, these changes were much milder than those reported for severely anemic fish.[53] Interestingly, KM and peripheral RBCs were normal in *gfi1aa*^{qmc551}*hom* fish (Figure 7C-E). This is consistent with our previous finding that qmc551:GFP is not expressed in KM RBCs.[37] Thus, although Gfi1aa and Gfi1b act together during primitive erythropoiesis, Gfi1b alone is important for adult erythropoiesis.

Gfi1aa/1b do not mediate the suppression of the hemangioblast transcription factor Npas4l/Cloche in primitive red blood cell progenitors

Our 20-hpf RNA-Seq data showed that Gfi1aa/1b-depleted prRBCs displayed reduced expression of the late erythroid transcription program (*slc4a1a*) and elevated levels of early erythroid (*zfp36l2*) and endothelial genes (*etv2*), gene expression changes that the subsequent WISH experiments revealed to reflect a delay in cellular differentiation. Forcing the suppression of EC genes in Gfi1aa-depleted embryos with an *etv2* MO[63,64] only partially restored *slc4a1a* expression levels (supplemental Figure 10), showing that this is only one aspect of Gfi1aa's role.

Our transcriptome analysis did not suggest that Gfi1aa/1b suppressed other mesodermal transcription programs or downregulated the hemangioblast TF Npas4l/Cloche in prRBCs (Figure 7G-H). To see whether this was also true at earlier stages, we performed WISH experiments on *gfi1aa*^{qmc551}/*gfi1b*^{qmc554} double-mutant embryos we derived in sufficiently large numbers from the identified double-mutant parents. These WISH data revealed that even at earlier stages, there was no ectopic expression of *myoD1*, *pax2a*, and *nkx2.5* in Gfi1aa/Gfi1b-depleted RBCs in the PLM (Figure 7I-J). We also found no evidence for an abnormal maintenance of npas4l/cloche expression in double-mutant prRBCs (Figure 7K-L). While at 13 hpf, the *npas4l/cloche* expression domain encompasses prRBCs and arterial EC progenitors (Figure 7K),[18] only the medial DA angioblasts retain this expression by 14 hpf (Figure 7L). *Hbbe1.1*-expressing prRBCs switch *npas4l/cloche* off in *wt* embryos. In double-mutant embryos, that was no different. *Npas4l/cloche* was downregulated, but the lack of *hbbe1.1* mRNA indicated that prRBC differentiation was delayed (Figure 7L). From these data, we conclude that Gfi1aa/1b-deficient mesodermal cells progress normally through early hemangioblast stages and into the erythroid cell lineage, where in the *wt*, first Gfi1aa and then Gfi1b are expressed to suppress EC and early erythroid genes to promote late erythroid differentiation at its normal speed.

Discussion

Cellular differentiation proceeds by step-wise progression through individual regulatory states hard-wired in the genomic DNA sequence.[65,66] Gene regulatory networks of transcription factors, under the influence of extracellular signals, act in subcircuits to define each of these regulatory states. Progression from one state to another involves the activation of the next subcircuit, as well as the suppression of previous and alternative ones in negative feed forward loops. Our RNA-Seq analysis identifies Gfi1aa and Gfi1b

Figure 6. (continued) and dorsal views of embryos are shown in panels E and K, respectively. Cohorts of embryos derived from the crosses indicated were stained in panels A-D. Examples of embryos with high and low gene expression are depicted. Bar charts summarize the genotyping data in panels A-C. In panel D, 6/96 22- to 23-hpf and 9/89 23- to 24-hpf embryos had very low *slc4a1a* expression. Genotyping 11 of these showed that all of them were *qmc551/qmc554* double-homozygous mutants. Embryos with slightly stronger staining turned out to be *gfi1aa*^{qmc551}*hom;gfi1b*^{qmc554}*het* carriers. A more comprehensive overview of the WISH data on the 23- to 24-hpf embryos is presented in supplemental Figure 5. In panel E, 98 2-day-old-embryos from an incross of *gfi1aa*^{qmc551}*het;gfi1b*^{qmc554}*het* parents were stained with *o*-dianisidine (*o*-dia.) for the presence of hemoglobin. Four embryos displayed reduced staining. Genotyping showed that they were double homozygous mutants. In panel F, 3-day-old embryos with normal (red arrow) and hypochromic (red arrowhead) prRBCs are shown. The bar charts summarize the genotyping results. (G) RBCs were isolated from 2- and 3-day-old *wt* and double-mutant embryos. Cells were fixed with methanol and stained with Giemsa. (H) The size of the RBC nuclei (n>15 cells per embryo) was determined with Image J for *wt* and *gfi1aa*^{qmc551}*;gfi1b*^{qmc554} double-mutant embryos at 2 and 3 dpf (n ≥ 10 embryos for every type of embryos and every stage). Average values per embryo are plotted. Mean values and standard deviations are indicated. A 1-way analysis of variance (ANOVA) test revealed that the differences between the mean values were statistically significant for the comparisons indicated (ANOVA test performed on GraphPad Prism: *$P < .05$; ***$P < .001$; ****$P < .0001$). (I) Fluorescent images of the trunk and tail of representative embryos with hypochromic (top) and normal (bottom) blood as shown in panel F. The genotypes of the representative embryos are shown. In panel J, *cmyb* WISH experiments on GFP-low (ie, *gfi1aa*^{qmc551}*het*, embryos from a *gfi1aa*^{qmc551}/*gfi1b*^{qmc554} double heterozygous incross) revealed no differences in staining between embryos. Genotyping revealed that 4 of the 24 embryos were *gfi1b*^{qmc554}*hom*. In panel K, 20 5-dpf embryos derived from a *gfi1b*^{qmc554}*het* incross were stained for the expression of the T-cell gene *rag1*. All embryos showed the same level of *rag1* expression, including the 5 *gfi1b*^{qmc554}*hom* embryos.

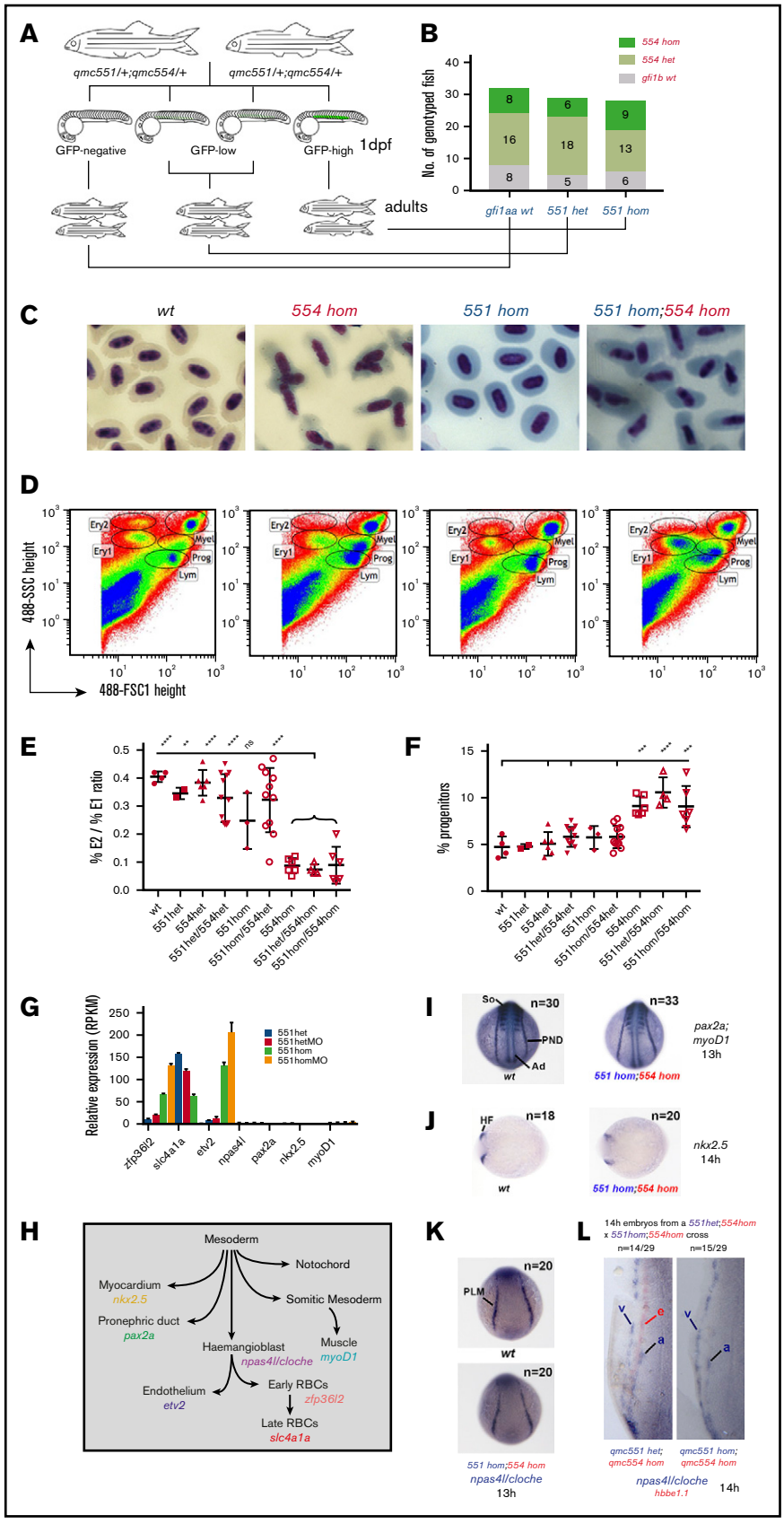

Figure 7.

as actors in a negative feed forward loop that suppresses the early erythroid, as well as the alternative EC regulatory states to promote late erythroid differentiation. Studying the kinetics of EC and erythroid gene expression in the synchronously developing prRBCs, our WISH experiments reveal that early cellular differentiation was not completely blocked, but delayed, in *gfi1aa/1b* mutant embryos. Additional mechanisms must exist that ensure developmental progression, albeit at a reduced speed. Its early onset of expression makes Gfi1aa the prominent player in early prRBC differentiation, a role that it later shares with Gfi1b. The prolonged maintenance of *gfi1aa* expression in *gfi1aa/gfi1b* mutants likely reflects delayed cellular maturation rather than the kind of auto- or cross-regulation that was reported in other contexts.[67-71] In the adult, Gfi1b alone is important for the formation of normal defRBCs. Their asynchronous development in the KM makes it difficult to examine whether their differentiation is delayed in the absence of Gfi1b.

The phenotype of our *gfi1aa/1b* double-mutant embryos is very similar to the phenotype of the lsd1-mutant zebrafish.[72] In particular, the early widespread *etv2* expression in the PLM and the late posterior restriction of EC gene expression suggest that *lsd1*-mutant prRBCs are not blocked, as suggested,[72] but delayed in differentiation, and that lysine-specific demethylase 1 (Lsd1) and Gfi1aa/1b act in the same pathway. Lsd1 is a histone demethylase that acts as corepressor and coactivator in a context-dependent manner.[73-75] During hematopoiesis, Lsd1 interacts with numerous TFs, including Gfi1 and Gfi1b.[76-78] Our data suggest that in prRBCs, Gfi1aa/1b are the TFs that take Lsd1 to its target genes, one of which is *etv2*.[72] Depletion of the endothelial TF Etv2 blocks ectopic endothelial gene expression and only slightly elevates *slc4a1a* expression in *gfi1aa*-mutant prRBCs.

The need to suppress EC genes in early prRBCs highlights the bipotent nature of the progenitor cells from which prRBCs arise. Whether PLM cells themselves are hemangioblasts or constitute a mix of angioblasts and erythroid progenitors derived from hemangioblasts is unclear. Lineage labeling studies have identified hemangioblasts during early gastrulation.[17] Blood and endothelial gene expression, however, commence after gastrulation and show considerable overlap in the PLM.[16,21-25,79-82] Expression of both gene sets relies on the TF Npas4l/Cloche,[23,79,81,83] which itself is expressed only from the end of gastrulation.[18] Notch and Wnt signaling appear to differentially bias the fate choice of hemangioblasts. Notch favors prRBC differentiation in nascent mesoderm,[20] whereas Wnt promotes endothelial development specifically in the PLM.[19] Our finding that Gfi1aa suppresses EC gene expression in prRBCs of the PLM implies that these prRBCs have only recently developed from hemangioblasts.

Our data confirm and extend our knowledge on the role of Gfi1/1b during erythropoiesis in the vertebrate embryo. *Gfi1b*-mutant mouse embryos display defects in primitive and definitive erythropoiesis. Snapshot analyses show that they carry prRBCs with immature morphology at embryonic day (E) 9.5-10.5, and lack all enucleated defRBCs at E14.[84] *Gfi1b*-mutant mice eventually die at E15.[84] *Gfi1/Gfi1b*-double-knockout mouse embryos die at E11 and display strongly reduced *βH1* and *βmajor* globin expression at E8.5,[85] suggesting a more severe defect in the development of prRBC and pre-defRBCs of the yolk sac. In the double mutants, pre-defRBCs, identified as $CD41^{+}$, Gfi1:GFP, and Gfi1b:GFP-expressing cells, fail to enter circulation and remain trapped in the yolk sac vasculature.[85] Reverse transcription PCR showed that they display elevated levels of several EC mRNAs, suggesting that mouse Gfi1/Gfi1b normally repress EC genes in yolk sac HECs as they undergo EHT.[85] Here, we show for the first time that Gfi1/Gfi1b also suppress EC genes in prRBCs as they arise from hemangioblasts. It is likely that the same is true in the mouse.

Although Gfi1/Gfi1b-depleted RBCs are abnormal in mouse and fish mutants, the consequences for the affected individuals are dramatically different. *Gfi1b*-single- and *Gfi1/Gfi1b*-double-mutant mice die in utero,[84,85] whereas mice with an erythroid-specific deletion of *Gfi1b* die perinatally.[86] Conditional deletion of *Gfi1b* in adult mouse bone marrow cells blocks erythropoiesis and is lethal within 3 weeks.[87] By contrast, single- and double-mutant zebrafish are viable. Their differential survival may reflect

Figure 7. Gfi1aa/1b do not mediate Npas4l/Cloche suppression in primitive red blood cells. (A-F) Gfi1b single- and Gfi1aa/1b double-mutant fish are viable but carry abnormal RBCs. (A) An incross of double heterozygous *gfi1aa*^{qmc551} and *gfi1b*^{qmc554} carriers provided GFP-negative, GFP-low, and GFP-high embryos in Mendelian ratios. These embryos were separated and grown up to adulthood. (B) Genotyping at 15 months revealed that *gfi1b wt*, *gfi1b*^{qmc554}*het*, and *gfi1b*^{qmc554}*hom* genotypes were represented in all 3 batches in Mendelian ratios (GraphPad Prism; χ-square tests: *P*[*wt*]>0.99; *P*[*het*]=.64, and *P*[*hom*]=.83). (C) Blood smears were prepared and stained with Giemsa. (D) The forward and side scatter profiles were analyzed for kidney marrow cells isolated from the fish that had been genotyped in panel B. The gating follows a published protocol.[53] (E) Relative abundance of 2 subpopulations of live erythrocytes, named Ery1 and Ery2, in the forward and side scatter profiles determined for the kidney marrow cells isolated from the fish genotyped in panel B. (F) Percentage of cells in the progenitor gate of the forward and side scatter profile of the kidney marrow cells isolated from the fish genotyped in panel B. (G-K) Gfi1aa/1b do not suppress the hemangioblast TF Npas4l/Cloche and TFs associated with other mesodermal cell fates. (G) Relative expression levels of selected genes in the 20 hpf prRBCs, as determined by RNA-Seq (see also Figures 1 and 2). The genes were selected as markers for particular cell fates and differentiation stages, as shown in panel H. The schematic diagram shown in panel H describes the relationship of selected cell lineages that arise from the nonaxial mesoderm of the zebrafish embryo. For the prRBC lineage, 2 genes were selected as early and late markers of prRBC differentiation, *zpf36l2* and *slc4a1a*, respectively. For each of the other lineages, a key transcription factor gene was selected as a marker for lineage specification. (I-L) Embryos were stained in WISH experiments. In panels I-L, embryos were derived from incrosses of *wt* parents and from crosses of *gfi1aa*^{qmc551}/*gfi1b*^{qmc554} double homozygous to *gfi1aa*^{qmc551}*het*;*gfi1b*^{qmc554}*hom* fish. Numbers of embryos provided on the panels correspond to the number of embryos in the batch used in the WISH experiments. A subset of these embryos was genotyped after the WISH staining. Representative embryos of known genotype are displayed. Posterior views of embryos are shown in panels I and K. Dorsal views are shown in panel J, with anterior pointing toward the left. The left-hand sides of the posterior two-thirds of flat-mounted embryos are shown in panel L. *Pax2a* is expressed in the pronephric duct (PND). *MyoD1* expression highlights the adaxial cells (Ad) and the forming muscle in the developing somites (So). *Nkx2.5* is expressed in the anterior bilateral heart fields (HF). At 13 hpf, *npas4l/cloche* is expressed in blood and in arterial endothelial progenitors in the PLM (K). At 14 hpf (L), *npas4l/cloche*-expressing cells are arranged in 2 stripes: a medial stripe of arterial (a) and a lateral stripe of future venous (v) angioblasts. *Hbbe1.1*-expressing prRBC progenitors are located next to the arterial stripe. These prRBCs lack *hbbe1.1* expression, but do not gain *npas4l/cloche* expression in the absence of Gfi1aa and Gfi1b.

obvious differences between extra- and intrauterine embryogenesis, differences in RBC biology or adult physiology that affect the fitness of the cells or the selection pressures they experience. Numerous examples show that gene essentiality is context-dependent.[88]

Our novel *gfi1b*-mutant lines show that definitive hematopoiesis proceeds normally in the absence of Gfi1b. Consistent with this, *gfi1aa*, and not *gfi1b*, is expressed in HECs of the vDA, and *gfi1ab* expression is triggered in its absence.[37] In the mouse, *Gfi1* and *Gfi1b* act redundantly in HSC formation[89] and maintenance.[90] Whether loss of all 3 Gfi1/Gfi1b TFs in zebrafish block HSC formation by interfering with EHT in the vDA or inhibit subsequent HSC maintenance remains to be examined.

Acknowledgments

The authors thank David Onion and Nicola Croxall for their help in flow cytometry. The authors also thank the 2017/18 third-year project students Harry Oughton, Iman Mustafa, Jenny Walsh, Kabilas Parameswaran, Maria Blasco Cabildo, and Sita Mall for their help in this project.

This work was supported by Medical Research Council grants (G0601134 and MR/J000841/1) (M.G.), an MRC PhD studentship (Y.H.), a University of Nottingham International PhD studentship (D.U.), and a Chinese Scholarship Council PhD studentship (Y.C.).

Authorship

Contribution: C.M., J.L.R., Y.H., D.U., S.M., Y.C., S.E., R.N.W., and M.G. performed experiments; F.S. and M.G. performed the bioinformatics; R.N.W. and M.G. conceived the study; M.G. prepared the manuscript; and C.M., J.L.R., Y.H., and R.N.W. critiqued the output for important intellectual content.

Conflict-of-interest disclosure: The authors declare no competing financial interests.

ORCID profiles: C.M., 0000-0002-3122-7502; J.L.R., 0000-0001-5868-3914; R.N.W., 0000-0003-2706-316X; M.G., 0000-0003-3763-0885.

Correspondence: Martin Gering, School of Life Sciences, University of Nottingham, Queen's Medical Centre, Nottingham NG7 2UH, United Kingdom; e-mail: martin.gering@nottingham.ac.uk.

References

1. Medvinsky A, Rybtsov S, Taoudi S. Embryonic origin of the adult hematopoietic system: advances and questions. *Development*. 2011;138(6):1017-1031.
2. Dzierzak E, Speck NA. Of lineage and legacy: the development of mammalian hematopoietic stem cells. *Nat Immunol*. 2008;9(2):129-136.
3. Frame JM, McGrath KE, Palis J. Erythro-myeloid progenitors: "definitive" hematopoiesis in the conceptus prior to the emergence of hematopoietic stem cells. *Blood Cells Mol Dis*. 2013;51(4):220-225.
4. Ciau-Uitz A, Monteiro R, Kirmizitas A, Patient R. Developmental hematopoiesis: ontogeny, genetic programming and conservation. *Exp Hematol*. 2014;42(8):669-683.
5. Huber TL, Kouskoff V, Fehling HJ, Palis J, Keller G. Haemangioblast commitment is initiated in the primitive streak of the mouse embryo. *Nature*. 2004;432(7017):625-630.
6. Yokomizo T, Ogawa M, Osato M, et al. Requirement of Runx1/AML1/PEBP2alphaB for the generation of haematopoietic cells from endothelial cells. *Genes Cells*. 2001;6(1):13-23.
7. Goldie LC, Lucitti JL, Dickinson ME, Hirschi KK. Cell signaling directing the formation and function of hemogenic endothelium during murine embryogenesis. *Blood*. 2008;112(8):3194-3204.
8. Frame JM, Fegan KH, Conway SJ, McGrath KE, Palis J. Definitive hematopoiesis in the yolk sac emerges from Wnt-responsive hemogenic endothelium independently of circulation and arterial identity. *Stem Cells*. 2016;34(2):431-444.
9. Chen MJ, Li Y, De Obaldia ME, et al. Erythroid/myeloid progenitors and hematopoietic stem cells originate from distinct populations of endothelial cells. *Cell Stem Cell*. 2011;9(6):541-552.
10. Yokomizo T, Dzierzak E. Three-dimensional cartography of hematopoietic clusters in the vasculature of whole mouse embryos. *Development*. 2010;137(21):3651-3661.
11. Boisset J-C, van Cappellen W, Andrieu-Soler C, Galjart N, Dzierzak E, Robin C. In vivo imaging of haematopoietic cells emerging from the mouse aortic endothelium. *Nature*. 2010;464(7285):116-120.
12. Zovein AC, Hofmann JJ, Lynch M, et al. Fate tracing reveals the endothelial origin of hematopoietic stem cells. *Cell Stem Cell*. 2008;3(6):625-636.
13. Gordon-Keylock S, Sobiesiak M, Rybtsov S, Moore K, Medvinsky A. Mouse extraembryonic arterial vessels harbor precursors capable of maturing into definitive HSCs. *Blood*. 2013;122(14):2338-2345.
14. de Bruijn MF, Speck NA, Peeters MC, Dzierzak E. Definitive hematopoietic stem cells first develop within the major arterial regions of the mouse embryo. *EMBO J*. 2000;19(11):2465-2474.
15. Chen W, Paradkar PN, Li L, et al. Abcb10 physically interacts with mitoferrin-1 (Slc25a37) to enhance its stability and function in the erythroid mitochondria. *Proc Natl Acad Sci USA*. 2009;106(38):16263-16268.
16. Gering M, Rodaway ARF, Göttgens B, Patient RK, Green AR. The SCL gene specifies haemangioblast development from early mesoderm. *EMBO J*. 1998;17(14):4029-4045.
17. Vogeli KM, Jin S-W, Martin GR, Stainier DYR. A common progenitor for haematopoietic and endothelial lineages in the zebrafish gastrula. *Nature*. 2006;443(7109):337-339.
18. Reischauer S, Stone OA, Villasenor A, et al. Cloche is a bHLH-PAS transcription factor that drives haemato-vascular specification. *Nature*. 2016;535(7611):294-298.

19. Hübner K, Grassme KS, Rao J, et al. Wnt signaling positively regulates endothelial cell fate specification in the Fli1a-positive progenitor population via Lef1. *Dev Biol*. 2017;430(1):142-155.

20. Lee CY, Vogeli KM, Kim S-H, et al. Notch signaling functions as a cell-fate switch between the endothelial and hematopoietic lineages. *Curr Biol*. 2009; 19(19):1616-1622.

21. Detrich HW III, Kieran MW, Chan FY, et al. Intraembryonic hematopoietic cell migration during vertebrate development. *Proc Natl Acad Sci USA*. 1995; 92(23):10713-10717.

22. Fouquet B, Weinstein BM, Serluca FC, Fishman MC. Vessel patterning in the embryo of the zebrafish: guidance by notochord. *Dev Biol*. 1997;183(1):37-48.

23. Liao W, Bisgrove BW, Sawyer H, et al. The zebrafish gene cloche acts upstream of a flk-1 homologue to regulate endothelial cell differentiation. *Development*. 1997;124(2):381-389.

24. Sumoy L, Keasey JB, Dittman TD, Kimelman D. A role for notochord in axial vascular development revealed by analysis of phenotype and the expression of VEGR-2 in zebrafish flh and ntl mutant embryos. *Mech Dev*. 1997;63(1):15-27.

25. Kohli V, Schumacher JA, Desai SP, Rehn K, Sumanas S. Arterial and venous progenitors of the major axial vessels originate at distinct locations. *Dev Cell*. 2013;25(2):196-206.

26. Al-Adhami MA, Kunz YW. Ontogenesis of haematopoietic sites in Brachydanio rerio (Hamilton-Buchanan) (Teleostei). *Dev Growth Differ*. 1977;19(2): 171-179.

27. Lawson ND, Scheer N, Pham VN, et al. Notch signaling is required for arterial-venous differentiation during embryonic vascular development. *Development*. 2001;128(19):3675-3683.

28. Jin S-W, Beis D, Mitchell T, Chen J-N, Stainier DYR. Cellular and molecular analyses of vascular tube and lumen formation in zebrafish. *Development*. 2005;132(23):5199-5209.

29. Gering M, Patient R. Hedgehog signaling is required for adult blood stem cell formation in zebrafish embryos. *Dev Cell*. 2005;8(3):389-400.

30. Burns CE, Traver D, Mayhall E, Shepard JL, Zon LI. Hematopoietic stem cell fate is established by the Notch-Runx pathway. *Genes Dev*. 2005;19(19): 2331-2342.

31. Bertrand JY, Chi NC, Santoso B, Teng S, Stainier DY, Traver D. Haematopoietic stem cells derive directly from aortic endothelium during development. *Nature*. 2010;464(7285):108-111.

32. Kissa K, Herbomel P. Blood stem cells emerge from aortic endothelium by a novel type of cell transition. *Nature*. 2010;464(7285):112-115.

33. Kissa K, Murayama E, Zapata A, et al. Live imaging of emerging hematopoietic stem cells and early thymus colonization. *Blood*. 2008;111(3):1147-1156.

34. Murayama E, Kissa K, Zapata A, et al. Tracing hematopoietic precursor migration to successive hematopoietic organs during zebrafish development. *Immunity*. 2006;25(6):963-975.

35. Jin H, Xu J, Wen Z. Migratory path of definitive hematopoietic stem/progenitor cells during zebrafish development. *Blood*. 2007;109(12):5208-5214.

36. Jin H, Sood R, Xu J, et al. Definitive hematopoietic stem/progenitor cells manifest distinct differentiation output in the zebrafish VDA and PBI. *Development*. 2009;136(4):647-654.

37. Thambyrajah R, Ucanok D, Jalali M, et al. A gene trap transposon eliminates haematopoietic expression of zebrafish Gfi1aa, but does not interfere with haematopoiesis. *Dev Biol*. 2016;417(1):25-39.

38. Dufourcq P, Rastegar S, Strähle U, Blader P. Parapineal specific expression of gfi1 in the zebrafish epithalamus. *Gene Expr Patterns*. 2004;4(1):53-57.

39. Wei W, Wen L, Huang P, et al. Gfi1.1 regulates hematopoietic lineage differentiation during zebrafish embryogenesis. *Cell Res*. 2008;18(6):677-685.

40. Cooney JD, Hildick-Smith GJ, Shafizadeh E, et al. Teleost growth factor independence (gfi) genes differentially regulate successive waves of hematopoiesis. *Dev Biol*. 2013;373(2):431-441.

41. Zweidler-Mckay PA, Grimes HL, Flubacher MM, Tsichlis PN. Gfi-1 encodes a nuclear zinc finger protein that binds DNA and functions as a transcriptional repressor. *Mol Cell Biol*. 1996;16(8):4024-4034.

42. Grimes HL, Chan TO, Zweidler-McKay PA, Tong B, Tsichlis PN. The Gfi-1 proto-oncoprotein contains a novel transcriptional repressor domain, SNAG, and inhibits G1 arrest induced by interleukin-2 withdrawal. *Mol Cell Biol*. 1996;16(11):6263-6272.

43. Tong B, Grimes HL, Yang TY, et al. The Gfi-1B proto-oncoprotein represses p21WAF1 and inhibits myeloid cell differentiation. *Mol Cell Biol*. 1998; 18(5):2462-2473.

44. van der Meer LT, Jansen JH, van der Reijden BA. Gfi1 and Gfi1b: key regulators of hematopoiesis. *Leukemia*. 2010;24(11):1834-1843.

45. Möröy T, Vassen L, Wilkes B, Khandanpour C. From cytopenia to leukemia: the role of Gfi1 and Gfi1b in blood formation. *Blood*. 2015;126(24): 2561-2569.

46. Westerfield M. The zebrafish book. A guide for the laboratory use of zebrafish (Danio rerio). Eugene: University of Oregon Press; 2000

47. Mortazavi A, Williams BA, McCue K, Schaeffer L, Wold B. Mapping and quantifying mammalian transcriptomes by RNA-Seq. *Nat Methods*. 2008;5(7): 621-628.

48. Miller JC, Tan S, Qiao G, et al. A TALE nuclease architecture for efficient genome editing. *Nat Biotechnol*. 2011;29(2):143-148.

49. Hwang WY, Fu Y, Reyon D, et al. Efficient genome editing in zebrafish using a CRISPR-Cas system. *Nat Biotechnol*. 2013;31(3):227-229.

50. Moreno-Mateos MA, Vejnar CE, Beaudoin J-D, et al. CRISPRscan: designing highly efficient sgRNAs for CRISPR-Cas9 targeting in vivo. *Nat Methods*. 2015;12(10):982-988.

51. Broadbent J, Read EM. Wholemount in situ hybridization of Xenopus and zebrafish embryos. *Methods Mol Biol*. 1999;127:57-67.

52. Gansner JM, Madsen EC, Mecham RP, Gitlin JD. Essential role for fibrillin-2 in zebrafish notochord and vascular morphogenesis. *Dev Dyn*. 2008;237(10):2844-2861.

53. Traver D, Paw BH, Poss KD, Penberthy WT, Lin S, Zon LI. Transplantation and in vivo imaging of multilineage engraftment in zebrafish bloodless mutants. *Nat Immunol*. 2003;4(12):1238-1246.

54. Anders S, Huber W. Differential expression analysis for sequence count data. *Genome Biol*. 2010;11(10):R106.

55. Kettleborough RNW, Busch-Nentwich EM, Harvey SA, et al. A systematic genome-wide analysis of zebrafish protein-coding gene function. *Nature*. 2013;496(7446):494-497.

56. Zhang XY, Rodaway ARF. SCL-GFP transgenic zebrafish: in vivo imaging of blood and endothelial development and identification of the initial site of definitive hematopoiesis. *Dev Biol*. 2007;307(2):179-194.

57. Paw BH, Davidson AJ, Zhou Y, et al. Cell-specific mitotic defect and dyserythropoiesis associated with erythroid band 3 deficiency. *Nat Genet*. 2003;34(1):59-64.

58. Liao EC, Paw BH, Peters LL, et al. Hereditary spherocytosis in zebrafish riesling illustrates evolution of erythroid beta-spectrin structure, and function in red cell morphogenesis and membrane stability. *Development*. 2000;127(23):5123-5132.

59. Wingert RA, Brownlie A, Galloway JL, et al. The chianti zebrafish mutant provides a model for erythroid-specific disruption of transferrin receptor 1. *Development*. 2004;131(24):6225-6235.

60. Shaw GC, Cope JJ, Li L, et al. Mitoferrin is essential for erythroid iron assimilation. *Nature*. 2006;440(7080):96-100.

61. Shafizadeh E, Paw BH, Foott H, et al. Characterization of zebrafish merlot/chablis as non-mammalian vertebrate models for severe congenital anemia due to protein 4.1 deficiency. *Development*. 2002;129(18):4359-4370.

62. Brownlie A, Donovan A, Pratt SJ, et al. Positional cloning of the zebrafish sauternes gene: a model for congenital sideroblastic anaemia. *Nat Genet*. 1998;20(3):244-250.

63. Sumanas S, Lin S. Ets1-related protein is a key regulator of vasculogenesis in zebrafish. *PLoS Biol*. 2006;4(1):e10.

64. Rowlinson JM, Gering M. Hey2 acts upstream of Notch in hematopoietic stem cell specification in zebrafish embryos. *Blood*. 2010;116(12):2046-2056.

65. Swiers G, Patient R, Loose M. Genetic regulatory networks programming hematopoietic stem cells and erythroid lineage specification. *Dev Biol*. 2006;294(2):525-540.

66. Howard ML, Davidson EH. cis-Regulatory control circuits in development. *Dev Biol*. 2004;271(1):109-118.

67. Doan LL, Porter SD, Duan Z, et al. Targeted transcriptional repression of Gfi1 by GFI1 and GFI1B in lymphoid cells. *Nucleic Acids Res*. 2004;32(8):2508-2519.

68. Vassen L, Okayama T, Möröy T. Gfi1b:green fluorescent protein knock-in mice reveal a dynamic expression pattern of Gfi1b during hematopoiesis that is largely complementary to Gfi1. *Blood*. 2007;109(6):2356-2364.

69. Vassen L, Fiolka K, Mahlmann S, Möröy T. Direct transcriptional repression of the genes encoding the zinc-finger proteins Gfi1b and Gfi1 by Gfi1b. *Nucleic Acids Res*. 2005;33(3):987-998.

70. Anguita E, Villegas A, Iborra F, Hernández A. GFI1B controls its own expression binding to multiple sites. *Haematologica*. 2010;95(1):36-46.

71. Huang D-Y, Kuo Y-Y, Chang Z-F. GATA-1 mediates auto-regulation of Gfi-1B transcription in K562 cells. *Nucleic Acids Res*. 2005;33(16):5331-5342.

72. Takeuchi M, Fuse Y, Watanabe M, et al. LSD1/KDM1A promotes hematopoietic commitment of hemangioblasts through downregulation of Etv2. *Proc Natl Acad Sci USA*. 2015;112(45):13922-13927.

73. Shi Y, Lan F, Matson C, et al. Histone demethylation mediated by the nuclear amine oxidase homolog LSD1. *Cell*. 2004;119(7):941-953.

74. Metzger E, Wissmann M, Yin N, et al. LSD1 demethylates repressive histone marks to promote androgen-receptor-dependent transcription. *Nature*. 2005;437(7057):436-439.

75. Wang J, Scully K, Zhu X, et al. Opposing LSD1 complexes function in developmental gene activation and repression programmes. *Nature*. 2007;446(7138):882-887.

76. Saleque S, Kim J, Rooke HM, Orkin SH. Epigenetic regulation of hematopoietic differentiation by Gfi-1 and Gfi-1b is mediated by the cofactors CoREST and LSD1. *Mol Cell*. 2007;27(4):562-572.

77. Hu X, Li X, Valverde K, et al. LSD1-mediated epigenetic modification is required for TAL1 function and hematopoiesis. *Proc Natl Acad Sci USA*. 2009;106(25):10141-10146.

78. Stadhouders R, Cico A, Stephen T, et al. Control of developmentally primed erythroid genes by combinatorial co-repressor actions. *Nat Commun*. 2015;6(1):8893.

79. Liao EC, Paw BH, Oates AC, Pratt SJ, Postlethwait JH, Zon LI. SCL/Tal-1 transcription factor acts downstream of cloche to specify hematopoietic and vascular progenitors in zebrafish. *Genes Dev*. 1998;12(5):621-626.

80. Brown LA, Rodaway AR, Schilling TF, et al. Insights into early vasculogenesis revealed by expression of the ETS-domain transcription factor Fli-1 in wild-type and mutant zebrafish embryos. *Mech Dev*. 2000;90(2):237-252.

81. Sumanas S, Jorniak T, Lin S. Identification of novel vascular endothelial-specific genes by the microarray analysis of the zebrafish cloche mutants. *Blood*. 2005;106(2):534-541.

82. Liu F, Walmsley M, Rodaway A, Patient R. Fli1 acts at the top of the transcriptional network driving blood and endothelial development. *Curr Biol*. 2008;18(16):1234-1240.

83. Stainier DY, Weinstein BM, Detrich HW III, Zon LI, Fishman MC. Cloche, an early acting zebrafish gene, is required by both the endothelial and hematopoietic lineages. *Development*. 1995;121(10):3141-3150.

84. Saleque S, Cameron S, Orkin SH. The zinc-finger proto-oncogene Gfi-1b is essential for development of the erythroid and megakaryocytic lineages. *Genes Dev*. 2002;16(3):301-306.

85. Lancrin C, Mazan M, Stefanska M, et al. GFI1 and GFI1B control the loss of endothelial identity of hemogenic endothelium during hematopoietic commitment. *Blood*. 2012;120(2):314-322.

86. Vassen L, Beauchemin H, Lemsaddek W, Krongold J, Trudel M, Möröy T. Growth factor independence 1b (gfi1b) is important for the maturation of erythroid cells and the regulation of embryonic globin expression. *PLoS One*. 2014;9(5):e96636.

87. Foudi A, Kramer DJ, Qin J, et al. Distinct, strict requirements for Gfi-1b in adult bone marrow red cell and platelet generation. *J Exp Med*. 2014;211(5): 909-927.

88. Rancati G, Moffat J, Typas A, Pavelka N. Emerging and evolving concepts in gene essentiality. *Nat Rev Genet*. 2018;19(1):34-49.

89. Thambyrajah R, Mazan M, Patel R, et al. GFI1 proteins orchestrate the emergence of haematopoietic stem cells through recruitment of LSD1. *Nat Cell Biol*. 2016;18(1):21-32.

90. Khandanpour C, Sharif-Askari E, Vassen L, et al. Evidence that growth factor independence 1b regulates dormancy and peripheral blood mobilization of hematopoietic stem cells. *Blood*. 2010;116(24):5149-5161.